Molecular Docking Appraisal of *Pleurotus ostreatus* Phytochemicals as Potential Inhibitors of PI3K/Akt Pathway for Breast Cancer Treatment

Bioinformatics and Biology Insights
Volume 19: 1–15

DOI: 10.1177/11779322251316864

Magdalene Eno Effiong[1,2], Mercy Bella-Omunagbe[1,2], Israel Sunmola Afolabi[1,3] and Shalom Nwodo Chinedu[1,3]

[1]Department of Biochemistry, College of Science and Technology, Covenant University, Ota, Nigeria. [2]Covenant Applied Informatics and Communication Africa Centre of Excellence (CApIC-ACE), Covenant University, Ota, Nigeria. [3]Covenant University Public Health and Wellbeing Research Cluster (CUPHWERC), Covenant University, Ota, Nigeria.

ABSTRACT

INTRODUCTION: Breast cancer (BC) is a heterogeneous disease involving a network of numerous extracellular signal transduction pathways. The phosphoinositide 3-kinase (PI3K)/serine/threonine kinase (Akt)/mechanistic target of rapamycin (mTOR) pathway is crucial for understanding the BC development. Phosphoinositide 3-kinase, phosphatase and tensin homolog (PTEN), mTOR, Akt, 3-phosphoinositide-dependent kinase 1 (PDK1), FoxO1, glycogen synthase kinase 3 (GSK-3), mouse double minute 2 (MDM2), H-Ras, and proapoptotic B-cell lymphoma 2 (BCL-2) family protein (BAD) proteins are key drivers of this pathway and potential therapeutic targets. *Pleurotus ostreatus* is an edible mushroom that is rich in flavonoids and phenols that can serve as potential inhibitors of proteins in the PI3K/Akt/mTOR pathway.

AIM: This study evaluated the anticancer properties of *P ostreatus* through a structure-based virtual screening of 22 biologically active compounds present in the mushroom.

METHOD: Model optimization was carried out on PI3K, PTEN, mTOR, Akt, PDK1, FoxO1, GSK-3, MDM2, H-Ras, and BAD proteins in the PI3K/Akt/mTOR pathway and molecular docking of compounds/control inhibitors in the binding pocket were simulated AutoDock Vina in PyRx. The drug likeness, pharmacokinetic, and pharmacodynamic features of prospective docking leads were all anticipated.

RESULT: Several potent inhibitors of the selected key driver proteins in PI3K/Akt/mTOR pathway were identified from *P ostreatus*. Ellagic acid with binding affinities of −8.0, −8.0, −8.1, −8.2, −6.2, and −7.1 kcal/mol on PI3K, Akt, PDK1, GSK-3, MDM2, and BAD, respectively, had better binding affinity compared with their reference drugs. Likewise, apigenin (−7.8 kcal/mol), chrysin (−7.8 kcal/mol), quercetin (−6.4 kcal/mol), and chlorogenic acid (−6.2 kcal/mol) had better binding affinities to PTEN, mTOR, FoxO1, and H-Ras proteins, respectively.

CONCLUSION: Ellagic acid, apigenin, luteolin, quercetin, chlorogenic acid, chrysin, and naringenin phytochemicals are seen as the better lead molecules due to their ability to strongly bind to the proteins under study in this pathway. Analogs of these compounds can also be designed as potential drugs.

KEYWORDS: molecular docking, drug targets, breast cancer, PI3K/Akt/mTOR pathway, *Pleurotus ostreatus*

RECEIVED: June 9, 2024. **ACCEPTED:** January 6, 2025.

TYPE: Research Article

FUNDING: The author(s) disclosed receipt of the following financial support for the research, authorship, and/or publication of this article: The authors are grateful to Covenant Applied Informatics and Communication—Africa Centre of Excellence (CApIC-ACE) and Covenant University Centre for Research Innovation and Discovery (CUCRID) for the funding.

DECLARATION OF CONFLICTING INTERESTS: The author(s) declared no potential conflicts of interest with respect to the research, authorship, and/or publication of this article.

CORRESPONDING AUTHOR: Magdalene Eno Effiong, Department of Biochemistry, College of Science and Technology, Covenant University, Canaanland, PMB 1023, 112233, Ota, Ogun State, Nigeria. Email: magdalene.effiongpgs@stu.cu.edu.ng

Introduction

Breast cancer (BC) is a highly complex and multifactorial disease involving a network of numerous extracellular signal transduction pathways, which contributes to it heterogeneity.[1,2] Extracellular signaling is a process where cells produce specific molecules that bind to other cells' receptors, activating intracellular pathways.[3] Cell signal transduction is crucial for cancer growth and development, with tumor cells exhibiting characteristics such as uncontrolled proliferation, genomic instability, and apoptosis evasion.[4,5] Modifications to various cell signaling pathways promote these processes, often due to mutations in oncogenes, mutated proteins, or inactivation of tumor suppressor genes.[6,7] Breast cancer cells have been subjected to various alterations, including calcium-sensitive receptors, hypoxia-inducible factor, and apoptotic cell mechanisms.[8,9] Estrogen receptor and human epidermal growth factor receptors are the most researched on which are often directly involved in promoting signaling of other pathways, highlighting the importance of signal integration and transduction processes in BC progression.[4,10]

The phosphoinositide 3-kinase (PI3K)/serine/threonine kinase (Akt)/mechanistic target of rapamycin (mTOR) complex is a crucial pathway for essential cellular activities like metabolism, growth, proliferation, apoptosis, and angiogenesis.[11,12] A

ligand binds to a cell-membrane receptor, activating PI3K and phosphorylating phosphatidylinositol 4,5-bisphosphate (PIP2), which recruits Akt and 3-phosphoinositide-dependent kinase 1 (PDK1) to the plasma membrane. This phosphorylation stimulates cell survival, growth, and proliferation.[13] PI3K/Akt/mTOR is a cell signaling pathway involved in growth, proliferation, survival, motility, metabolism, and immune response regulation.[14] It is associated with various diseases and syndromes, including tuberous sclerosis, Parkinson's disease, and vascular diseases. The dysregulation of this pathway is linked to cancer hallmarks like uncontrolled proliferation, genomic instability, and metabolic reprogramming and is implicated in up to 60% of human tumors.[4] PI3K/Akt/mTOR activation is also a major cause of cancer cell resistance to antitumor therapies.[15] Therefore, the PI3K/Akt/mTOR pathway is crucial for understanding the disease's development, potential therapeutic targets, and prognostic and diagnostic value in BC patients.

Current research has focused on the discovery of multiple PI3K inhibitors that can be used alone or in combination with other drugs; however, much work still remains to be done.[16-21] The pursuit of natural bioactives as potent PI3K/Akt/mTOR pathway inhibitors is justified by the limitations observed in synthetic inhibitors. Despite the development of various PI3K inhibitors, including first-generation, second-generation, and dual PI3K/mTOR inhibitors, their therapeutic efficacy is often compromised.[21-23] Tumor cell mutations, compensatory feedback mechanisms, and significant toxicity have hindered the success of these synthetic agents.[24] Consequently, research has shifted toward using these inhibitors in combination with other drugs to enhance their effectiveness, although challenges persist.[25-27] Natural bioactives present a promising alternative due to their potential to offer higher specificity, reduced toxicity, and the ability to overcome resistance mechanisms inherent in tumor cells.[28] This approach could lead to more effective and safer cancer therapies, addressing the shortcomings of current synthetic inhibitors.

P ostreatus is an edible mushroom that is rich in nutrients, antioxidants and diverse phytochemicals such as flavonoids, phenols, and saponins among others.[29,30] These bioactive compounds increase its biological and medicinal significance. Reports by Effiong et al,[30] have shown that *P ostreatus* contains apigenin, benzoic acid, caffeic acid, chlorogenic acid, chrysin, cinnamic acid, ellagic acid, ferulic acid, gallic acid, luteolin, naringenin, phenylacetic acid, quercetin, rutin trihydrate, salicylic acid, syringic acid, vanillic acid, and 3,4-dimethoxybenzoic acid which have high antioxidant, anticancer, and anti-inflammatory properties. These natural bioactives can be explored in relation to their ability to influence the PI3K/Akt signal transduction by interacting with key drivers of the pathway, thereby serving as promising drug agents in BC treatment. Therefore, this study evaluates the inhibition potential of identified phytochemicals present in *P ostreatus* against selected key drivers of the PI3K/Akt pathway with the aim of identifying novel inhibitors and drug promising agents.

Materials and Methods

Protein retrieval and preparation

The 3-dimensional structure of the proteins involved in PI3K pathway of BC: PI3K (IE8Y), phosphatase and tensin homolog (PTEN) (1D5R), mTOR (1AUE), Akt (3CQW), PKD1 (1H1W), H-Ras (121P), FoxO1 (3CO6), glycogen synthase kinase 3 (GSK-3) (7SXF), MDM2 (1RV1), and proapoptotic B-cell lymphoma 2 (BCL-2) family protein (BAD) (7Q16) was obtained from the RCSB Protein Data Bank (PDB) (https://www.rcsb.org/). The proteins were prepared with Chimera 1.17.3. This includes the removal of co-crystallized ligands and other nonstandard residues, the addition of hydrogen atoms and charges, and the energy minimization of the structures.

Ligand library generation and preparation

The ligands used were the flavonoids and phenol compounds identified by High Performance Liquid Chromatography (HPLC) of *P ostreatus* (Figure 1). The canonical smiles and 3-dimensional structure of these ligands were obtained from PubChem (https://pubchem.ncbi.nlm.nih.gov/) to create the ligand library. Known inhibitors of the proteins under study were added to the library to serve as reference compounds (Table 1).

Molecular docking

The molecular docking was carried out using AutoDock Vina in PyRx.[31,32] Furthermore, the interactions formed after docking were visualized using Discovery Studio 2021.

ADMET and pharmacologic properties of the compounds

The Absorption, Distribution, Metabolism, Excretion and Toxicity (ADMET) properties of the best-performing compounds were predicted using pkCSM server according to the method described by Xiong et al[33] and Effiong et al.[34]

Molecular dynamics simulation

The study used molecular dynamics (MD) to simulate biological behavior, including water molecules and lipid membranes using the methods described by Owoloye et al.[35] Newton's equations were used to calculate the movements of water, ions, small molecules, macromolecules, and complex systems. The study focused on the pattern of recognition of ligand-protein or protein-protein complexes, focusing on structural motions driven by temperature and solute/solvent.[36] Desmond Schrodinger was conducted to do 100-ns MD simulations, whereas docking experiments were used to generate protein-ligand complexes for MD simulations. The Protein Preparation Wizard of Maestro Schrodinger Suite 2017 was used to preprocess the protein-ligand complex, and all systems were

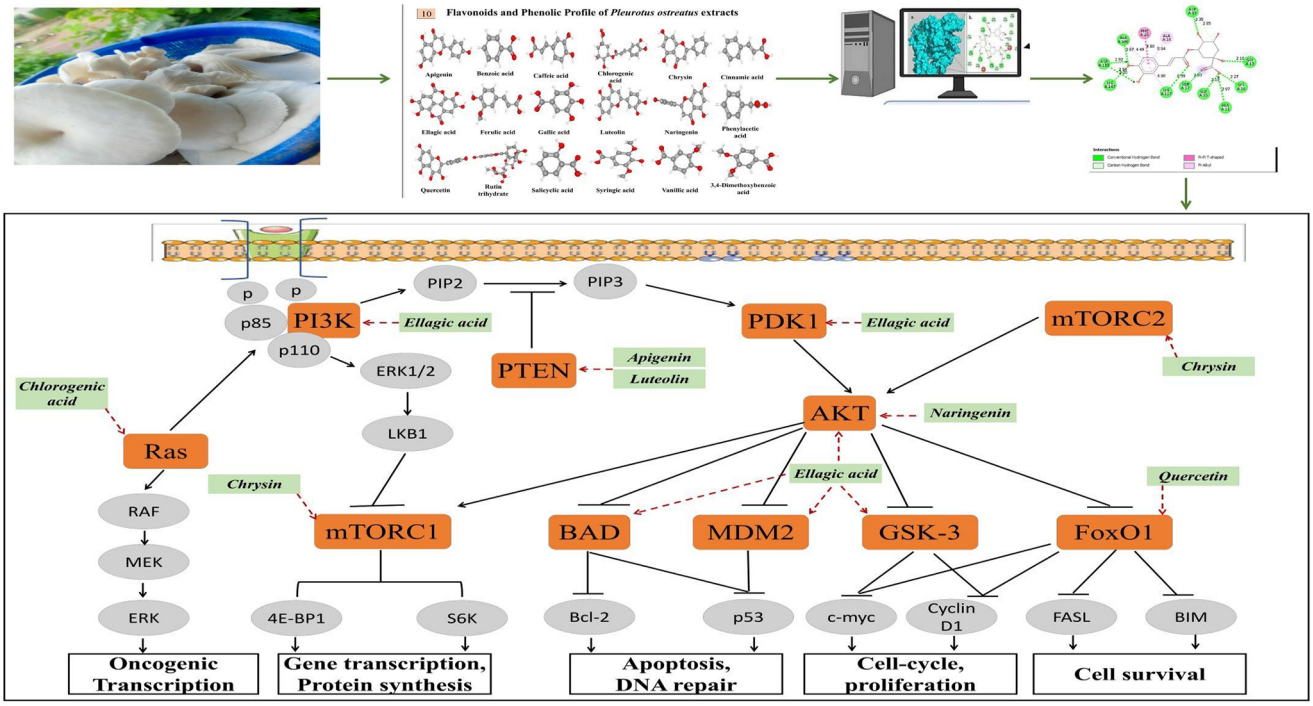

Figure 1. Graphical abstract.

Table 1. Known inhibitors of the proteins under study.

S/N	PROTEINS	STANDARD DRUGS/INHIBITORS
1	PI3K	Wortmannin and LY294002
2	PTEN	bpV(phen), bpV(pic), VO-OHpic, and SF1670
3	mTOR	Torin 1, torin 2, vistusertib, and rapamycin
4	Akt	LY2780301
5	PDK1	MP7, PKM2 activator 6
6	H-Ras	Tipifarnib
7	FoxO1	AS1842856
8	GSK-3	Indirubin, tideglusib, CHIR99021
9	MDM2	Brigimadlin, idasanutlin
10	BAD	N-cyclopentyl-3-((4-(2,3-dichlorophenyl) piperazin-1-yl) (2-hydroxyphenyl) methyl) benzamide

created using the System Builder tool.[37-39] The simulation was conducted using the OPLS_2005 force field,[40] with the solvent model with an orthorhombic box as the transferable intermolecular interaction potential 3 points (TIP3P). Counter ions were introduced to neutralize the models, and the Number of Particles, Pressure and Temperature (NPT) ensemble with 300 K temperature and one atmospheric pressure was chosen for full simulation using the Martyna-Tuckerman-Klein Barostat.[41] The models were equilibrated before the simulation, and the trajectories at a total run of 100 ns were carried out. The stability of the simulations was assessed by calculating the root mean square deviation (RMSD) of the protein and ligand over time before assessing the mean square fluctuation (RMSF) and protein-ligand interactions.

Results

Molecular docking

Molecular docking predicts the binding affinity and the structure formed by the protein-ligand complex.[42,43] The information on the docking scores of the ligands to the proteins is in Supplemental File 1. The visualization of the interactions formed by the best ligands and proteins is found in Supplemental File 2.

Screening of phytochemicals against PI3K. Among the 22 phytochemical compounds, the top 5 were ellagic acid, chrysin, quercetin, luteolin, and apigenin and classified by their low binding affinities. The binding affinity range among these compounds was −8 to −8.7 kcal/mol. The binding affinity of the standard inhibitors was −9.7 and −8 kcal/mol for LY294002 and wortmannin, respectively (Table 2). All the top ligands outperformed wortmannin. Ellagic acid with the lowest binding affinity from the top ligands formed hydrogen bonds with TYR867, ASP964, and VAL882. Other interactions include Pi-Sulfur with MET953; Pi-Sigma with ILE963, Pi-Pi T-shaped with TYR867, and Pi-Alkyl with ILE879, ILE831, MET80, ILE963, and MET953 (Figure 2).

Table 2. Binding affinities for top phytochemicals against PI3K.

S/N	LIGAND	BINDING AFFINITY (KCAL/MOL)
1	LY294002	−9.7
2	Ellagic acid	−8.7
3	Chrysin	−8.5
4	Quercetin	−8.4
5	Luteolin	−8.3
6	Apigenin	−8.0
7	Wortmannin	−8.0

Table 3. Binding affinities for top phytochemicals against PTEN.

S/N	LIGAND	BINDING AFFINITY (KCAL/MOL)
1	SF1670	−8.4
2	Apigenin	−8.0
3	Luteolin	−8.0
4	Chlorogenic acid	−7.8
5	Naringenin	−7.8
6	Chrysin	−7.8
7	bpV(phen)	−6.4
8	VO-OHpic	−5.2

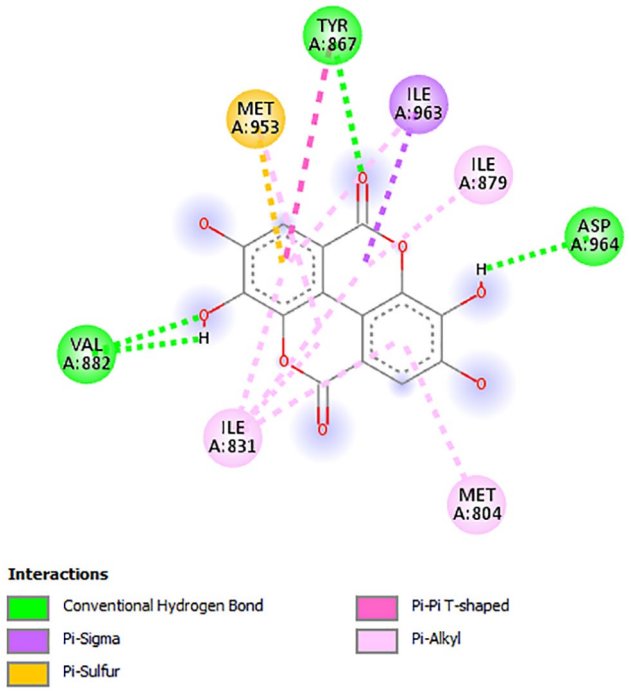

Figure 2. 2D visualization of ligand interaction in the PI3K-ellagic acid complex.

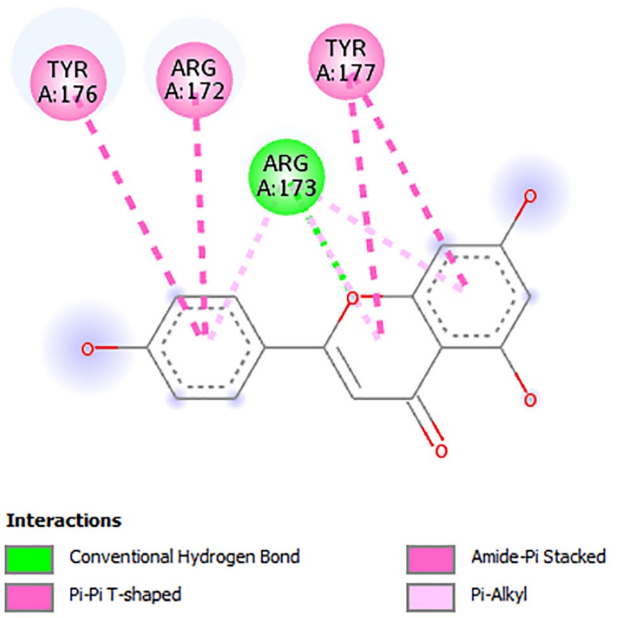

Figure 3. 2D visualization of ligand interaction in the PTEN-apigenin complex.

Screening of phytochemicals against PTEN. Among the 22 phytochemical compounds, the top 5 were apigenin, luteolin, chlorogenic acid, naringenin, and chrysin and classified by their low binding affinities. The binding affinity range among these compounds was −7.8 to −8 kcal/mol. The binding affinity of the standard inhibitors was −8.4, −6.4, and −5.2 kcal/mol for SF1670, bpV(phen), and VO-OHpic, respectively (Table 3). Based on the binding affinity, all the top ligands outperformed the inhibitors bpV(phen) and VO-OHpic but not SF1670. Apigenin with the lowest binding affinity from the top ligands formed a hydrogen bond with ARG173. Other interactions formed include Pi-Alkyl with ARG173 and Pi-Pi T-shaped/Amide Pi-stacked with TYR176, ARG172, and TYR177 (Figure 3).

Screening of phytochemicals against mTOR. Among the 22 phytochemical compounds, the top ligands were chrysin, luteolin, apigenin, naringenin, and quercetin and classified by their low binding affinities. The binding affinity range among these compounds was −7.8 to −8.4 kcal/mol. The binding affinity of the standard inhibitors was −8.9, −7.6, −6.9, and −6.6 kcal/mol for torin 2, vistusertib, torin 1, and rapamycin, respectively (Table 4). Based on the binding affinity, all the top ligands outperformed the inhibitors vistusertib, torin 1, and rapamycin but not torin 2. Apigenin with the lowest binding affinity from the top ligands formed a hydrogen bond with ASP2103 and a van der Waals interaction with GLU2033 and Pi-Pi Stacked/Amide Pi-Stacked with PHE2040 and LEU2032 (Figure 4).

Table 4. Binding affinities for top phytochemicals against mTOR.

S/N	LIGAND	BINDING AFFINITY (KCAL/MOL)
1	Torin 2	−8.9
2	Chrysin	−8.4
3	Luteolin	−8.2
4	Apigenin	−8.0
5	Naringenin	−7.9
6	Quercetin	−7.8
7	Vistusertib	−7.6
8	Torin 1	−6.9
9	Rapamycin	−6.6

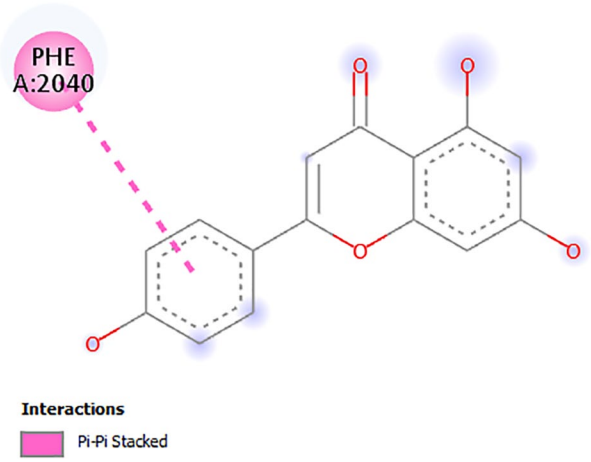

Figure 4. 2D visualization of ligand interaction in the mTOR-apigenin complex.

Screening of phytochemicals against Akt. Among the 22 phytochemical compounds, the top ligands were ellagic acid, naringenin, quercetin, luteolin, and chlorogenic acid and classified by their low binding affinities. The binding affinity range among these compounds was −8 to −8.3 kcal/mol (Table 5). The binding affinity of the standard inhibitor, LY2780301, was −10.3 kcal/mol. Ellagic acid with the lowest binding affinity from the top ligands formed hydrogen bonds with ASP292 and LYS179. Other interactions include Pi-Sulfur with MET227 and MET281; Pi-Sigma with VAL164 and THR291; and Pi-Alkyl with ALA177, MET227, MET281, and VAL164 (Figure 5).

Screening of phytochemicals against PDK1. Among the 22 phytochemical compounds, the top ligands were ellagic acid, chrysin, naringenin, luteolin, and chlorogenic acid and classified by their low binding affinities. The binding affinity range among these compounds was −8.1 to −8.6 kcal/mol

Table 5. Binding affinities for top phytochemicals against Akt.

S/N	LIGAND	BINDING AFFINITY (KCAL/MOL)
1	LY2780301	−10.3
2	Ellagic acid	−8.3
3	Naringenin	−8.1
4	Quercetin	−8.1
5	Luteolin	−8.1
6	Chlorogenic acid	−8.0

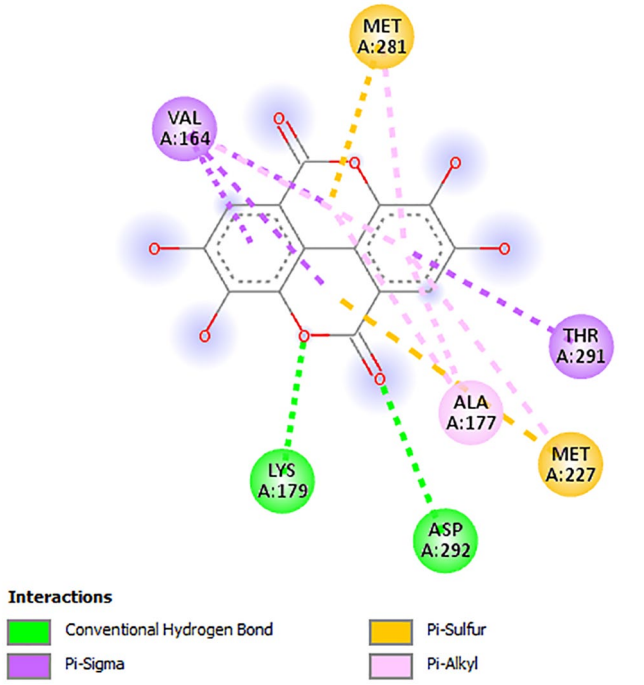

Figure 5. 2D visualization of ligand interaction in the Akt-ellagic acid complex.

(Table 6). The binding affinity of the standard inhibitors was 10.7 and −9.6 kcal/mol for MP7 and PKM2 activator 6, respectively. Ellagic acid with the lowest binding affinity from the top ligands formed hydrogen bonds with LYS111 and SER160. Other interactions include Pi-Sigma with VAL96, and Pi-Alkyl with VAL96, LEU212, ALA109, and ALA162 (Figure 6).

Screening of phytochemicals against FoxO1. Among the 22 phytochemical compounds, the top ligands were quercetin, luteolin, ellagic acid, chlorogenic acid, and naringenin and classified by their low binding affinities. The binding affinity range among these compounds was −6.4 to −6.1 kcal/mol (Table 7). The binding affinity of the standard inhibitor, AS1842856, was −5.8 kcal/mol. Based on the binding affinity, all the top ligands outperformed the inhibitor, AS1842856. Quercetin with the

Table 6. Binding affinities for top phytochemicals against PDK1.

S/N	LIGAND	BINDING AFFINITY (KCAL/MOL)
1	MP7	−10.7
2	PKM2 activator 6 (compound Z10)	−9.6
3	Ellagic acid	−8.6
4	Chrysin	−8.3
5	Naringenin	−8.2
5	Luteolin	−8.2
6	Chlorogenic acid	−8.1

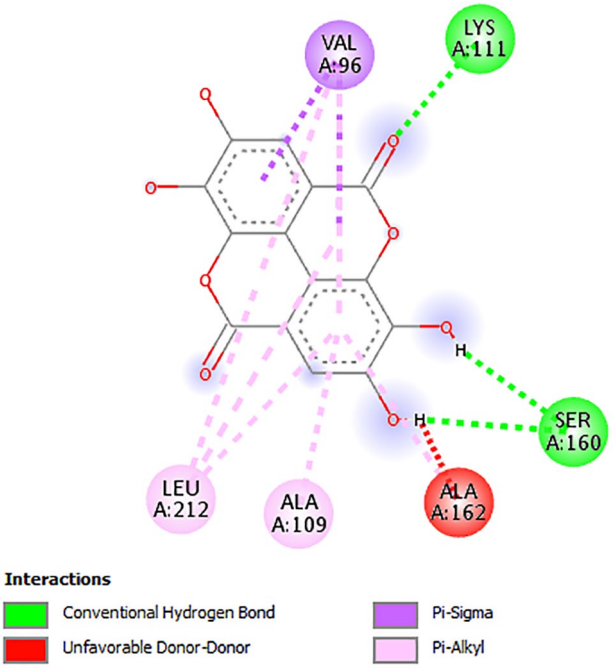

Figure 6. 2D visualization of ligand interaction in the PDK1-ellagic acid complex.

lowest binding affinity from the top ligands formed hydrogen bonds with GLU178, GLN185, and GLU188, and a carbon-hydrogen bond with SER176. Other interactions include Pi-Sigma and Pi-Akyl with LEU181 (Figure 7).

Screening of phytochemicals against GSK-3. Among the 22 phytochemical compounds, the top ligands were ellagic acid, quercetin, apigenin, and luteolin and classified by their low binding affinities (Table 8). The binding affinity range among these compounds was −8.2 to −8.3 kcal/mol. The standard inhibitors' binding affinity was −8.7, −8.6, and −8.2 kcal/mol for indirubin, tideglusib, and CHIR99021, respectively. Based on the binding affinity, all the top ligands outperformed the inhibitor, CHIR99021, but not indirubin and tideglusib.

Table 7. Binding affinities for top phytochemicals against FoxO1.

S/N	LIGAND	BINDING AFFINITY (KCAL/MOL)
1	Quercetin	−6.4
2	Luteolin	−6.2
3	Ellagic acid	−6.2
4	Chlorogenic acid	−6.1
5	Naringenin	−6.1
6	AS1842856	−5.8

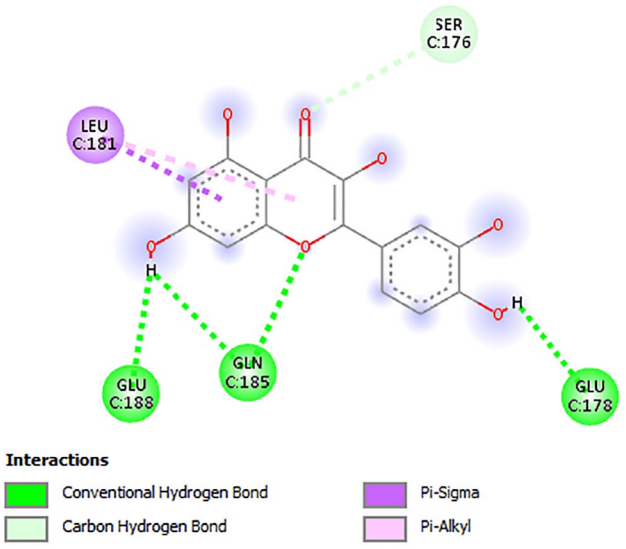

Figure 7. 2D visualization of ligand interaction in the FOXO1-quercetin complex.

Ellagic acid with the lowest binding affinity from the top ligands formed hydrogen bonds with VAL198 and ASP263. Other interactions include Pi-Sulfur with CYS262; Pi-Sigma with LEU251; and Pi-Alkyl with VAL173, LEU195, ALA146, CYS262, LYS148, and VAL133 (Figure 8).

Screening of phytochemicals against MDM2. Among the 22 phytochemical compounds, the top ligands were ellagic acid, chrysin, luteolin, chlorogenic acid, and naringenin and classified by their low binding affinities (Table 9). The binding affinity range among these compounds was −6.2 to −6.7 kcal/mol. The standard inhibitors' binding affinity was −9.3 and −7.1 kcal/mol, respectively. Based on the binding affinity, none of the top ligands outperformed the inhibitors. Ellagic acid with the lowest binding affinity from the top ligands formed hydrogen bonds with ASP68, GLU69, and TYR67 and a carbon-hydrogen bond with LEU66. It also formed Pi-Pi Stacked interactions with TYR76 (Figure 9).

Screening of phytochemicals against H-Ras. Among the 22 phytochemical compounds, the top ligands were chlorogenic acid, luteolin, ellagic acid, apigenin, and quercetin and classified

Table 8. Binding affinities for top phytochemicals against GSK-3.

S/N	LIGAND	BINDING AFFINITY (KCAL/MOL)
1	Tideglusib	−8.7
2	Indirubin	−8.6
3	Ellagic acid	−8.3
4	Quercetin	−8.2
5	Apigenin	−8.2
6	Luteolin	−8.2
7	CHIR99021	−8.2

Table 9. Binding affinities for top phytochemicals against MDM2.

S/N	LIGAND	BINDING AFFINITY (KCAL/MOL)
1	Brigimadlin	−9.3
2	Idasanutlin	−7.1
3	Ellagic acid	−6.7
4	Chrysin	−6.6
5	Luteolin	−6.5
6	Chlorogenic acid	−6.2
7	Naringenin	−6.2

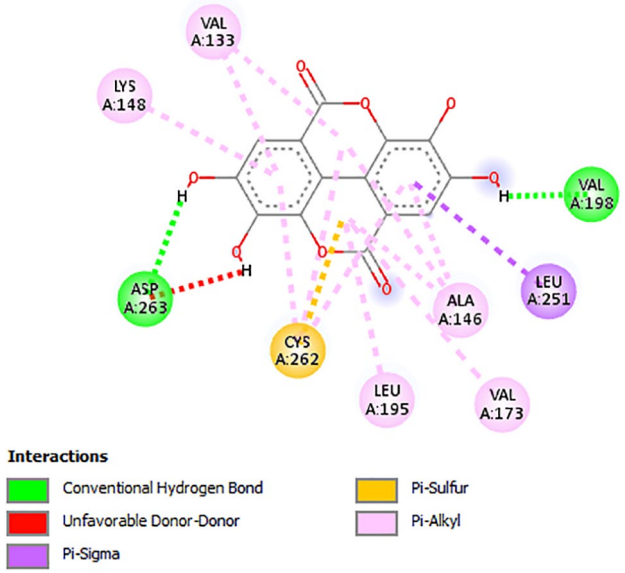

Figure 8. 2D visualization of ligand interaction in the GSK-3-ellagic acid complex.

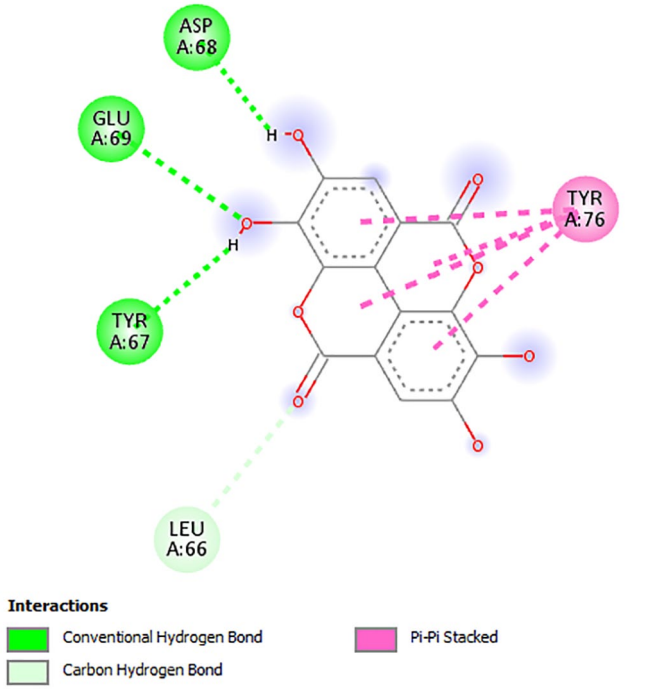

Figure 9. 2D visualization of ligand interaction in the MDM2-ellagic acid complex.

by their low binding affinities (Table 10). The binding affinity range among these compounds was −9.5 to −8.6 kcal/mol. The binding affinity of the standard inhibitor, tipifarnib, was −9.2 kcal/mol. Based on the binding affinity, only chlorogenic acid outperformed tipifarnib. Chlorogenic acid with the lowest binding affinity from the top ligands formed hydrogen bonds with ASP119, LYS147, ALA146, LYS117, SER17, GLY15, ALA11, LYS16, GLY13, and ASP33. It also formed a carbon-hydrogen bond with ASP33, a Pi-Alkyl interaction with ALA18, LYS117, and ALA146 and a Pi-Sigma interaction with PHE28 (Figure 10).

Screening of phytochemicals against BAD. Among the 22 phytochemical compounds, the top ligands were ellagic acid, quercetin, chlorogenic acid, apigenin, and luteolin and classified by their low binding affinities (Table 11). The binding affinity range among these compounds was −7.1 to −6.6 kcal/mol. The binding affinity of the standard inhibitor N-cyclopentyl-3-((4-(2,3-dichlorophenyl) piperazin-1-yl) (2-hydroxyphenyl) methyl) benzamide (NPB) was −7.8 kcal/mol. Based on the binding affinity, none of the top ligands outperformed NPB. Ellagic acid with the lowest binding affinity from the top ligands formed hydrogen bonds with GLU180, ASN224, TYR128, and ARG56. It formed a Pi-Sulfur interaction with ARG127, Pi-Sigma, and Pi-Alkyl interactions with VAL176 and ARG127 (Figure 11).

Pharmacologic properties of compounds

The pharmacologic properties of selected hit compounds, ellagic acid, apigenin, quercetin, and chlorogenic acid, are depicted in Table 12. The water solubility (log M/L) was all

Table 10. Binding affinities for top phytochemicals against H-Ras.

S/N	LIGAND	BINDING AFFINITY (KCAL/MOL)
1	Chlorogenic acid	−9.5
2	Tipifarnib	−9.2
3	Luteolin	−8.8
4	Ellagic acid	−8.8
5	Apigenin	−8.7
6	Quercetin	−8.6

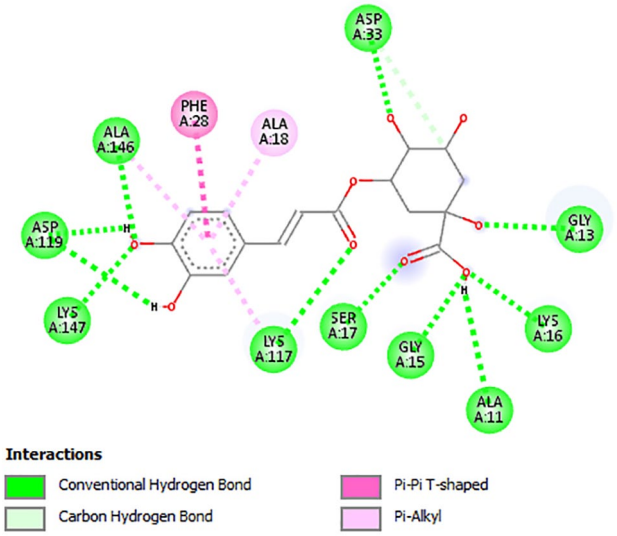

Figure 10. 2D visualization of ligand interaction in the chlorogenic acid in complex with H-Ras.

negative values. Likewise, negative results were observed for blood-brain barrier (BBB) penetrability for all compounds. A high intestinal absorption was predicted for all compounds except chlorogenic acid, which reported a low intestinal absorption. All the compounds were P-glycoprotein substrates (Table 12). As seen in Figure 12, the boiled egg shows that except for the Topological Polar Surface Area (TPSA) of chlorogenic acid and the LogP of apigenin, the compound parameters are all in the acceptable range for a drug.

Cytochrome P450 potentials of the compounds

The inhibitory properties of the ellagic acid, apigenin, quercetin, and chlorogenic acid on cytochrome P450 (CYP) isoforms are contained in Table 13. None of the compounds were able to inhibit CYP3A4, CYP2D6, and CYP2C9; likewise, none of the compounds were substrates of CYP2D6 and CYP3A4. All compounds except chlorogenic acid were able to inhibit CYP1A2. Only apigenin and quercetin were able to inhibit CYP2C9.

Table 11. Binding affinities for top phytochemicals against BAD.

S/N	LIGAND	BINDING AFFINITY (KCAL/MOL)
1	N-cyclopentyl-3-((4-(2,3-dichlorophenyl) piperazin-1-yl) (2-hydroxyphenyl) methyl) benzamide	−7.8
2	Ellagic acid	−7.1
3	Quercetin	−7.0
4	Chlorogenic acid	−6.6
5	Apigenin	−6.6
6	Luteolin	−6.6

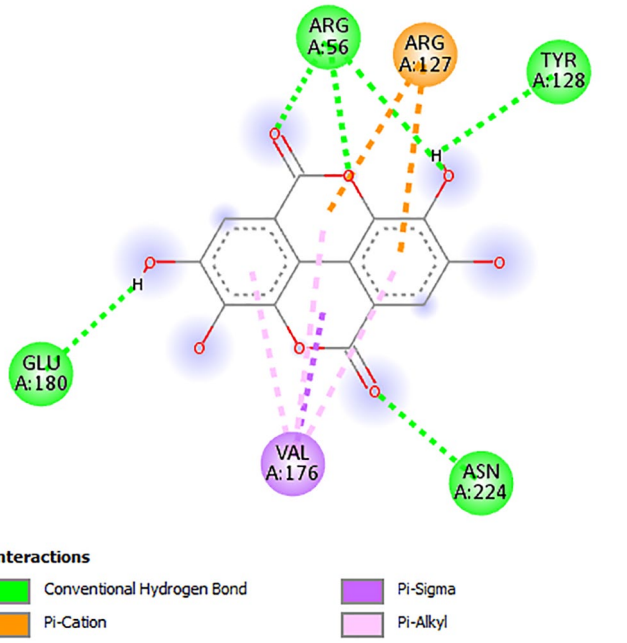

Figure 11. 2D visualization of ligand interaction in the BAD-ellagic acid complex.

Excretion and toxicity properties of the compounds

The excretion and toxicity studies of the selected compounds were examined as shown in Table 14. The compounds showed no AMES toxicity and hepatotoxicity. None of the compounds were inhibitors of human ether-à-go-go-related gene (hERG) I and hERG II inhibitor.

Molecular dynamics simulation

The MD simulation of ellagic acid was carried out on PI3K and Akt. The selected ligands were tested for conformational stability within the receptor's binding pocket. We studied the protein-ligand root mean square deviation (RMSD), protein root mean square fluctuation (RMSF), ligand RMSF, protein secondary structure, protein-ligand interactions, and ligand

Table 12. The absorption and distribution properties of the selected hits.

COMPOUNDS	WATER SOLUBILITY (LOG M/L)	INTESTINAL ABSORPTION	P-GLYCOPROTEIN SUBSTRATE	P-GLYCOPROTEIN I INHIBITOR	P-GLYCOPROTEIN II INHIBITOR	BBB PERMEABILITY (LOG BB)	CNS PERMEABILITY (LOG PS)
Ellagic acid	−3.181	86.684	Yes	No	No	−1.272	−3.533
Apigenin	−3.329	93.250	Yes	No	No	−0.734	−2.061
Quercetin	−2.925	77.207	Yes	No	No	−1.098	−3.065
Chlorogenic acid	−2.449	36.377	Yes	No	No	−1.407	−3.856

torsion profile. The RMSD is the average deviation in the displacement of a collection of atoms relative to a reference frame for a particular frame. Ellagic acid-Akt complex (lig-fit-prot) reached equilibrium at 58 ns. However, the equilibrium was not maintained until the conclusion of the evolution (100 ns) and ended at 62 ns, with lowest and maximum values of 0.60 and 3.00 Å, respectively (Figure 13A and B). However, the ellagic acid-PI3K complex (lig-fit-prot) attained equilibrium after the first 8 ns and held it until the end. The ellagic acid-PI3K complex (lig-fit-prot) achieved equilibrium after 8 ns and held it until the conclusion of the evolution (100 ns), with minimum and maximum values of 2.60 and 3.80 Å, respectively (Figure 13A and B).

The Cα atoms in the ellagic acid-Akt (Figure 13A) and ellagic acid-PI3K (Figure 13B) complexes showed constant variation after 1.8 and 3.4 Å, which lasted throughout the model. The equilibrium in the Cα atoms of the ellagic acid-PI3K complex lasted 90 ns (10-100 ns), whereas the equilibrium in the ellagic acid-Akt complex only lasted 4 ns (58-60 ns).

The RMSF describes local variations in the protein chain (Figure 13C and D). Local variations in the Akt and PI3K amino acid residues were examined over a 100-ns simulated run duration. Figure 13C and D shows a maximum loop region fluctuation of 5.4 Å across all models. Interestingly, there was a significant variation in the loop regions when comparing within models. The amino acid residues in Akt and PI3K models fluctuated between 0.5 to 4.0 Å and 0.6 to 6.0 Å, respectively.

Ellagic acid complex with lead compounds (E: Akt, 3CWQ; F: PI3K, 1E8Y): percentage of protein-ligand interactions observed over a 100-ns simulation run duration. The stacked bar charts illustrate the various forms of interactions between the ligands and the ellagic acid complex. The legend above displays the kind of interactions that occurred using the color code. The colors green, blue, purple, and red indicate hydrogen bonds, water bridges, hydrophobic bonds, and ionic bonds, respectively. Protein-ligand interactions were tracked throughout the simulation (Figures 13E and F).

Hydrogen bonds are vital in protein-ligand binding. In the ellagic acid-Akt complex, the conserved residues that generated hydrogen bond contacts were Lys158, Lys179, Glu228, Ala230, and Asp292, while in the ellagic acid-PI3K complex, they were Lys421, Leu475, Asn522, Arg614, Gln646, Glu649, Arg679, and Lys683. Hydrophobic contacts also developed between Val164, Ala177, and Met281 in the ellagic acid-Akt complex, as well as between Ile420, Val645, Ala676, and Lys683 in the ellagic acid-PI3K complex. Ionic bonds were only found in the ellagic acid-Akt complex generated by the Asp 292 residue; the ellagic acid-PI3K complex did not have ionic bonds. The simulation findings also showed that amino acid residues can be conserved by forming water bridges. The ellagic acid-Akt complex created water bridges with 12 of the 23 amino

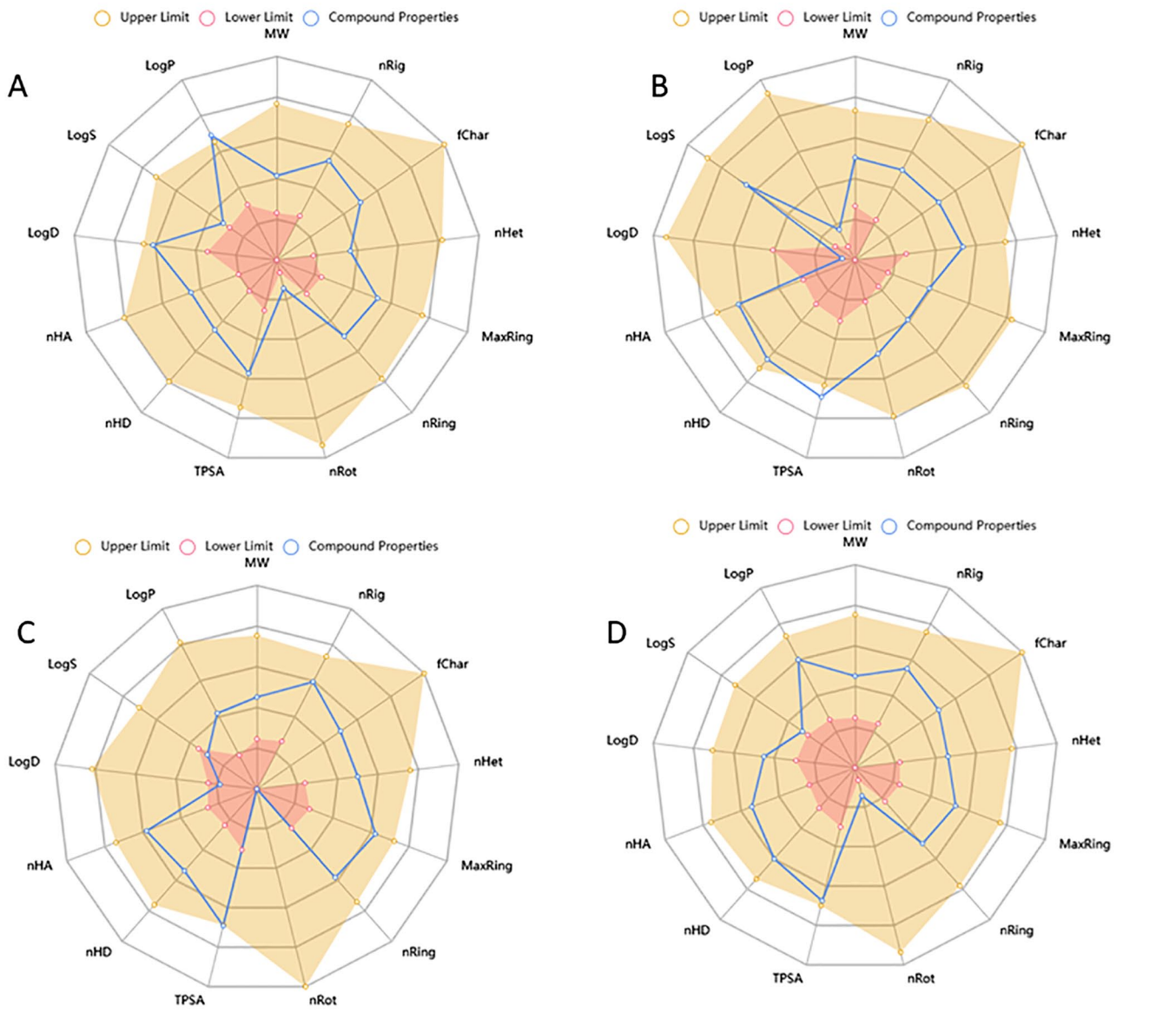

Figure 12. Radar charts generated by ADMETlab 2.0 tool with the chemical space of apigenin (A), chlorogenic acid (B), ellagic acid (C), and quercetin (D) on the upper and lower limits of crucial features for the drug likeness.

Table 13. The metabolism properties of the hits.

COMPOUNDS	CYP2D6 SUBSTRATE	CYP3A4 SUBSTRATE	CYP1A2 INHIBITOR	CYP2C19 INHIBITOR	CYP2C9 INHIBITOR	CYP2D6 INHIBITOR	CYP3A4 INHIBITOR
Ellagic acid	No	No	Yes	No	No	No	No
Apigenin	No	No	Yes	Yes	No	No	No
Quercetin	No	No	Yes	No	No	No	No
Chlorogenic acid	No	No	No	No	No	No	No

Table 14. Excretion and toxicity properties.

COMPOUNDS	TOTAL CLEARANCE (LOG ML/MIN/KG)	AMES TOXICITY	MAX TOLERATED DOSE (LOG MG/KG/DAY)	HERG I INHIBITOR	HERG II INHIBITOR	ORAL RAT ACUTE TOXICITY (MOL/KG)	HEPATOTOXICITY
Ellagic acid	0.537	No	0.476	No	No	2.399	No
Apigenin	0.566	No	0.328	No	No	2.450	No
Quercetin	0.407	No	0.499	No	No	2.471	No
Chlorogenic acid	0.307	No	−0.134	No	No	1.973	No

Abbreviations: hERG, human ether-à-go-go-related gene.

acid residues, including Leu156, Lys158, Thr160, Lys179, Glu198, Thr211, Ala230, Glu228, Glu234, Asp292, Tyr437, and Asp439. The water bridges generated in the ellagic acid-PI3K complex involved 15 of the 28 amino acid residues, which are Arg359, Ile420, Lys421, Leu423, Leu475, Arg477, Asn522, Gln601, Arg614, Glu638, Asn639, Ala642, Asp674, Arg679, and Lys683.

Discussion

HPLC analysis of *P ostreatus* has revealed a wealth of phenols, flavonoids, and unidentified saponins in its extracts. These compounds have potential anticancer properties, such as preventing cancer cell proliferation through mechanisms like cell cycle interruption and apoptosis induction.[44,45] However, the exact mechanisms underlying these effects remain elusive, and their specific impact on BC is scarcely explored. To fully harness the therapeutic potential of *P ostreatus*, *in silico* analysis was carried out to elucidate their molecular targets, and evaluate their efficacy in BC with respect to the PI3K/Akt/mTOR pathway.

The PI3K/Akt/mTOR pathway plays a crucial role in BC development as it is linked to a number of cancer markers. The PI3K/Akt/mTOR pathway is a complex network of proteins that regulates cell growth, survival, and proliferation.[14,46] The selected proteins in this study which consists of PI3K, PTEN, mTOR, Akt, PDK1, FoxO1, GSK-3, MDM2, H-Ras, and BAD play crucial roles in the activation of the PI3K/Akt/mTOR pathway enabling it to elucidate its downstream effects.[14] Overactivation of these proteins, which is often caused by phosphatidylinositol-4,5-bisphosphate (PIK3CA) gene mutations, promotes cell proliferation, survival, and migration, all of which contribute to BC progression.[47,48] PTEN, a tumor suppressor, acts as an antagonist to PI3K, inhibiting excessive PI3K signaling. mTOR, a Akt, regulates cell proliferation, survival, and protein synthesis.[11] Akt, key regulator protein in this pathway, encourages cell survival, proliferation, growth, angiogenesis, and metastasis. Overactivation of PDK1 leads to increased Akt activity, which promotes cancer.[11] FoxO1, a transcription factor involved in cell cycle arrest, apoptosis, and glucose metabolism, is also affected by Akt phosphorylation.[46] Overexpression of MDM2, a ubiquitin ligase that targets p53, can lower p53 levels, hence promoting cancer. Mutations in H-Ras may activate the PI3K pathway, which contributes to cancer.[47,48]

The bioactive compounds identified in *P ostreatus* include 2,5-dihydroxybenzoic acid, caffeic acid, phenylacetic acid, trans-cinnamic acid, quercetin, naringenin, chrysin, 3,4-dimethoxybenzoic acid, gallic acid, 4-hydroxybenzoic acid, salicylic acid, p-coumaric acid, rutin hydrate, o-coumaric acid, benzoic acid, chlorogenic acid, luteolin, 4-methoxycinnamic acid, and other 6 unidentified flavonoid compounds. Gallic acid, syringic acid, and ferulic acid have been reported to reduce proliferation and angiogenesis in BC cells by decreasing the phosphorylation of mTOR and Akt proteins in the PI3K/Akt/mTOR pathway.[49,50] Quercetin and apigenin inhibit the activation of Akt by increasing phosphatases activity and decreasing kinases activity, resulting in the suppression of mTOR signaling, cell growth, and evasion of apoptosis.[51-54] Most of the phenolic and flavonoid compounds identified have been reported to modulate the PI3K/Akt/mTOR pathway by interaction with the Akt, mTOR, and PI3K proteins, among others. This could be as a result of their high antioxidant, anti-inflammatory, anti-proliferative, and anticancer properties.

The *in silico* evaluation of the interaction between the bioactive compounds in *P ostreatus* and selected proteins in the PI3K/Akt/mTOR pathway revealed the potential of these compounds as candidates for BC treatment. The best hits' binding affinities were lower than the reference drugs indicating a high-affinity binding. Postscreening analysis was used to identify the type of interactions and bond lengths between the different compounds and the selected proteins. Ellagic acid is an ellagitannin that inhibits various signaling pathways involved in cancer cell proliferation and survival. It also improves DNA repair and inhibits enzymes that enable cancer cells to evade cell death.[55] Ellagic acid was found to be a top ligand for 6 out of the 10 selected proteins in the PI3K/Akt/mTOR pathway. It outperformed the reference drugs of PI3K, Akt, PDK1, GSK-3, MDM2, and BAD proteins, indicating that they are promising drug agents (Figure 1). These findings are similar to the reports of Mohammed Saleem and Selim,[56]

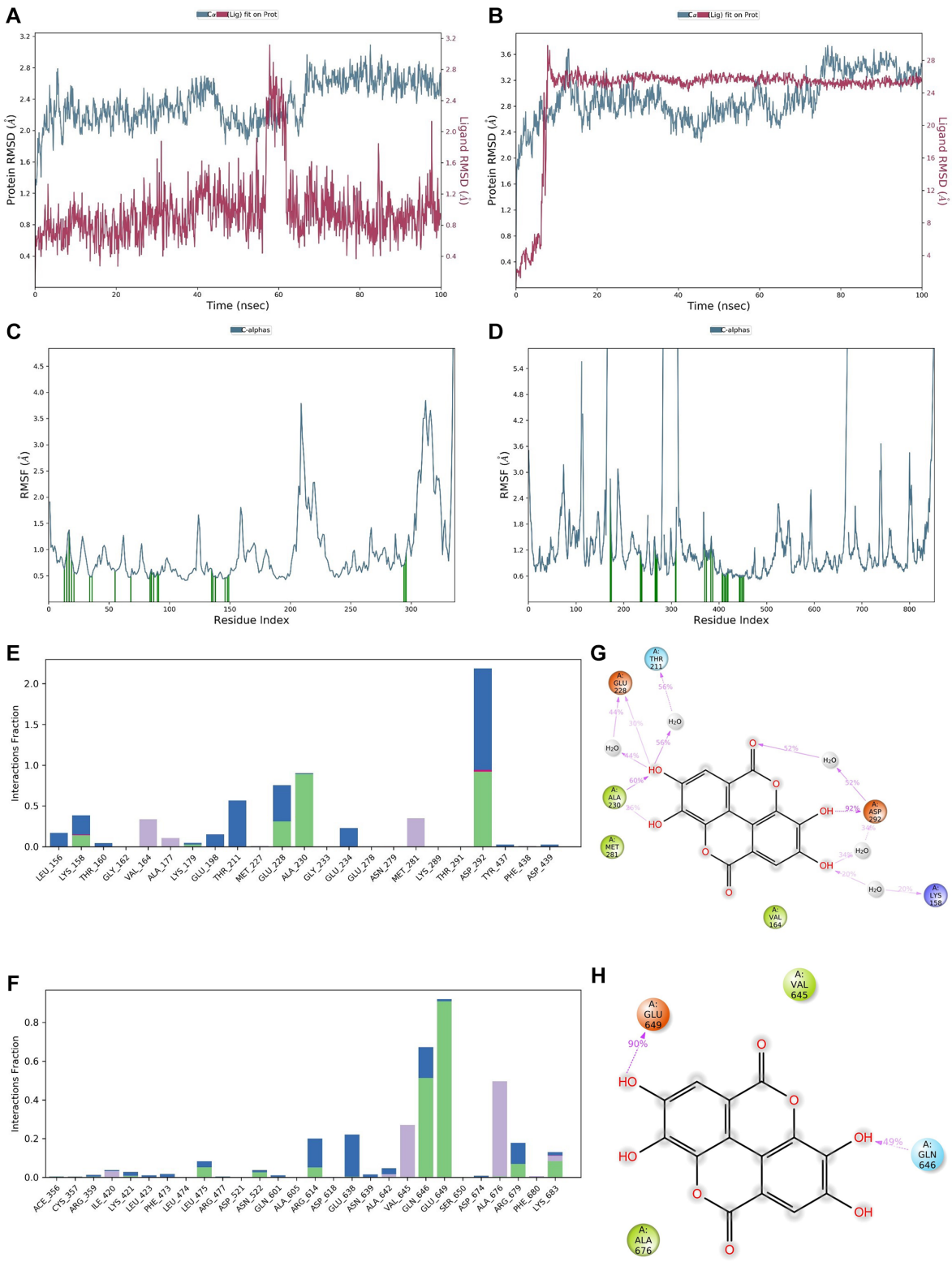

Figure 13. (A) Line plot illustrating the progression of RMSD during MD simulations of the ellagic acid complex with Akt (3CWQ). The left frame displays the RMSD value for ellagic acid—Cα, whereas the right frame displays the ligand's RMSD value. Lig-fit-lig shows the RMSD of a ligand that has been aligned and measured in its reference (first) conformation. (B) Line plot illustrating the progression of RMSD during MD simulations of the ellagic acid complex with PI3K (1E8Y). The left frame displays the RMSD value for ellagic acid—Cα, whereas the right frame displays the ligand's RMSD value. Lig-fit-lig shows the RMSD of a ligand that has been aligned and measured in its reference (first) conformation. (C) The root mean square fluctuation (RMSF) describes local variations in the protein chain (Akt, 3CWQ). (D) The root mean square fluctuation (RMSF) describes local variations in the protein chain (PI3K, 1E8Y). (E) The stacked bar charts illustrate the various forms of interactions between the Akt (3CWQ) and the ellagic acid complex. (F) The stacked bar charts illustrate the various forms of interactions between the PI3K, (1E8Y) and the ellagic acid complex. (G) 2D representation of MD simulations of ellagic acid complex and Akt (3CWQ). (H) 2D representation of MD simulations of ellagic acid complex and PI3K (1E8Y).

Zhao et al,[57] Wang et al,[58] and Vanella et al,[59] with respect to prostate cancer, colon cancer, glioblastoma, and prostate cancer cell lines, respectively. Other phytocompounds, such as apigenin, chrysin, quercetin, and chlorogenic acid, were top ligands of PTEN, mTOR, FoxO1, and H-Ras proteins, respectively, with better binding affinities compared with their reference drugs (Figure 1). These reports are in correlation with reports of Olayiwola and Gollahon,[28] and Čižmáriková et al,[55] on the chemopreventive and therapeutic abilities of natural compounds in BC.

The absorption and distribution characteristics of 4 bioactive compounds, ellagic acid, apigenin, quercetin, and chlorogenic acid, were examined. These characteristics are critical for maximizing their pharmacokinetics, particularly when employed for therapeutic purposes.[35] Water solubility is an important factor, as apigenin and ellagic acid are less soluble in water, which can reduce their absorption in the gastrointestinal tract and overall bioavailability when supplied orally. This is similar to reports by Kaur et al., Hu et al., Zuccari et al., Elendran et al., Chen et al., and Pais et al. [60-65] Another important attribute is intestinal absorption, which apigenin and ellagic acid exhibit at comparatively high rates, implying greater potential bioavailability when taken orally.[64,65] Quercetin has intermediate absorption, but chlorogenic acid has the lowest absorption, indicating restricted oral bioavailability. All 4 chemicals are P-glycoprotein (P-gp) substrates, which mean they are likely to be removed from cells via the P-gp transporter.[66,67] Apigenin has the highest BBB permeability among the compounds, suggesting a greater likelihood of crossing into the brain, making it potentially useful for CNS-related applications.[68] Ellagic acid, quercetin, and chlorogenic acid have significantly decreased BBB permeability, indicating their poor efficacy for Central Nervous System (CNS) uses unless permeability enhancers are included.[68]

The interaction of ellagic acid, apigenin, quercetin, and chlorogenic acid with CYP enzymes, which are crucial in drug metabolism, was examined. These enzymes affect drug processing and interactions with other compounds.[69,70] Ellagic acid, apigenin, and quercetin act as CYP1A2 inhibitors, whereas chlorogenic acid does not inhibit any of these enzymes. The inhibition activity of ellagic acid, apigenin, and quercetin may limit their use in combination with certain medications. Apigenin also inhibits CYP2C19, which can alter drug metabolism, leading to higher systemic concentrations and increased side effects risk.[71] Ellagic acid and quercetin do not inhibit this enzyme, suggesting fewer potential interactions. None of the compounds inhibit CYP2C9, CYP2D6, or CYP3A4 enzymes, which play critical roles in drug metabolism. This lack of inhibition reduces the risk of metabolic disruptions or drug-drug interactions with medications metabolized by these enzymes.[71] These metabolism properties provide insights into how these compounds might be metabolized in the body and their potential for combination therapies.

The study examined the excretion and toxicity properties of 4 bioactive compounds: ellagic acid, apigenin, quercetin, and chlorogenic acid. The compounds tested negative for AMES toxicity, indicating they do not cause DNA mutations and are unlikely to have mutagenic or carcinogenic effects.[72,73] Quercetin had the highest maximum tolerated dose (MTD), suggesting it can be administered at higher doses without significant toxicity. However, chlorogenic acid showed a negative MTD value, suggesting a lower tolerated dose, potentially limiting its use due to toxicity concerns at higher doses. No compounds inhibited hERG potassium channels, suggesting they do not pose a risk of cardiotoxicity. Oral rat acute toxicity measured the acute toxicity of the compounds when administered orally to rats, with higher values representing lower toxicity. Hepatotoxicity, the potential of a compound to cause liver damage, was not identified in any of the compounds.

The MD simulations of ellagic acid with the proteins phosphoinositide-3-kinase (PI3K) and Akt indicated significant differences in stability and interactions. The ellagic acid-PI3K complex achieved a more stable and consistent equilibrium, but the ellagic acid-Akt complex reached equilibrium later and only held it for 4 ns before becoming unstable again. This indicates that ellagic acid has a more permanent connection with PI3K, but the contact with Akt is more transitory and unstable. The Cα atom fluctuations confirmed these findings, with the ellagic acid-PI3K complex exhibiting steady fluctuations throughout the simulation, maintaining equilibrium for 90 ns. The ellagic acid-Akt complex demonstrated short-term equilibrium, lasting only 4 ns, with higher fluctuations (3.4 Å). Phosphoinositide 3-kinase has a more constant structural backbone (Cα atoms) than Akt, suggesting that ellagic acid fits better in its binding pocket. The RMSF analysis indicated significant local variations along the protein chains, with both complexes' loop regions demonstrating remarkable flexibility. Both complexes created hydrogen bonds, hydrophobic interactions, and water bridges; however, the distribution and types of interactions differed. The ellagic acid-PI3K complex created more constant water bridges, possibly contributing to the overall stability of the interaction. Furthermore, the ellagic acid-Akt combination demonstrated ionic bonding, which was lacking in the PI3K complex.

Conclusions

The key findings of this study reveal that various phytochemicals have the potential to inhibit the different genes of the PI3K pathway of BC. Phytochemicals such as ellagic acid, apigenin, luteolin, quercetin, chlorogenic acid, chrysin, and naringenin are seen as the better lead molecules due to their ability to strongly bind to the proteins under study in this pathway. Ellagic acid, apigenin, quercetin, and chlorogenic acid showed favorable excretion and toxicity properties, with moderate

clearance rates, no mutagenic activity, acceptable MTDs, low acute oral toxicity, and no hepatotoxicity or cardiotoxicity concerns. Molecular dynamics (MD) simulation study of ellagic acid-Akt and ellagic acid-PI3K complexes highlights significant differences in their binding dynamics. Ellagic acid binds more stably to PI3K, as shown by faster equilibrium accomplishment, persistent RMSD stability, and strong protein-ligand interactions. However, its interaction with Akt is less stable, with shorter equilibrium periods and more oscillations. Therefore, analogs of these compounds can also be designed as potential drugs. *In vivo* studies should be carried out to validate these findings.

Author Contributions

All authors conceptualized this research. Experiments, data analysis, and writing of original draft were carried out by Effiong Magdalene Eno and Mercy Bella-Omunagbe. Methodology validation and writing (review and editing) were carried out by Israel Sunmola Afolabi and Shalom Nwodo Chinedu.

Ethical Approval

Ethical approval was not required for this study. The study did not involve any human or animal subjects.

ORCID iDs

Magdalene Eno Effiong https://orcid.org/0000-0001-7250-2323
Mercy Bella-Omunagbe https://orcid.org/0000-0001-8190-4455

Data Availability

Data are available on request from the corresponding author.

Supplemental Material

Supplemental material for this article is available online.

REFERENCES

1. Feng Y, Spezia M, Huang S, et al. Breast cancer development and progression: risk factors, cancer stem cells, signaling pathways, genomics, and molecular pathogenesis. *Genes Dis*. 2018;5:77-106. doi:10.1016/j.gendis.2018.05.001
2. Testa U, Castelli G, Pelosi E. Breast cancer: a molecularly heterogenous disease needing subtype-specific treatments. *Med Sci*. 2020;8:18. doi:10.3390/medsci8010018
3. Nair A, Chauhan P, Saha B, Kubatzky KF. Conceptual evolution of cell signaling. *Int J Mol Sci*. 2019;20:3292. doi:10.3390/ijms20133292
4. Ortega MA, Fraile-Martínez O, Asúnsolo Á, Buján J, García-Honduvilla N, Coca S. Signal transduction pathways in breast cancer: the important role of PI3K/Akt/mTOR. *J Oncol*. 2020;2020:9258396. doi:10.1155/2020/9258396
5. Fu D, Hu Z, Xu X, Dai X, Liu Z. Key signal transduction pathways and crosstalk in cancer: biological and therapeutic opportunities. *Transl Oncol*. 2022;26:101510. doi:10.1016/j.tranon.2022.101510
6. Kontomanolis EN, Koutras A, Syllaios A, et al. Role of oncogenes and tumor-suppressor genes in carcinogenesis: a review. *Anticancer Res*. 2020;40:6009-6015. doi:10.21873/anticanres.14622.
7. Chen L, Liu S, Tao Y. Regulating tumor suppressor genes: post-translational modifications. *Signal Transduct Target Ther*. 2020;5:90. doi:10.1038/s41392-020-0196-9
8. Kozal K, Krześlak A. The role of hypoxia-inducible factor isoforms in breast cancer and perspectives on their inhibition in therapy. *Cancers*. 2022;14:4518. doi:10.3390/cancers14184518
9. Ji X, Lu Y, Tian H, Meng X, Wei M, Cho WC. Chemoresistance mechanisms of breast cancer and their countermeasures. *Biomed Pharmacother*. 2019;114:108800. doi:10.1016/j.biopha.2019.108800
10. Alataki A, Dowsett M. Human epidermal growth factor receptor-2 and endocrine resistance in hormone-dependent breast cancer. *Endocr Relat Cancer*. 2022;29:R105-R122. doi:10.1530/ERC-21-0293
11. Peng Y, Wang Y, Zhou C, Mei W, Zeng C. PI3K/Akt/mTOR pathway and its role in cancer therapeutics: are we making headway? *Front Oncol*. 2022;12:819128. doi:10.3389/fonc.2022.819128
12. Glaviano A, Foo ASC, Lam HY, et al. PI3K/AKT/mTOR signaling transduction pathway and targeted therapies in cancer. *Mol Cancer*. 2023;22:539-551. doi:10.1186/s12943-023-01827-6
13. He Y, Sun MM, Zhang GG, et al. Targeting PI3K/Akt signal transduction for cancer therapy. *Signal Transduct Target Ther*. 2021;6:425. doi:10.1038/s41392-021-00828-5
14. Miricescu D, Totan A, Stanescu-Spinu II, Badoiu SC, Stefani C, Greabu M. PI3K/AKT/mTOR signaling pathway in breast cancer: from molecular landscape to clinical aspects. *Int J Mol Sci*. 2021;22:1-24. doi:10.3390/ijms22010173
15. Dong C, Wu J, Chen Y, Nie J, Chen C. Activation of PI3K/AKT/mTOR pathway causes drug resistance in breast cancer. *Front Pharmacol*. 2021;12:628690. doi:10.3389/fphar.2021.628690
16. Tufail M, Hu JJ, Liang J, et al. Predictive, preventive, and personalized medicine in breast cancer: targeting the PI3K pathway. *J Transl Med*. 2024;22:15. doi:10.1186/s12967-023-04841-w
17. Yang L, Shi P, Zhao G, et al. *Targeting Cancer Stem Cell Pathways for Cancer Therapy*. Springer; 2020. doi:10.1038/s41392-020-0110-5
18. Zhong L, Li Y, Xiong L, et al. Small molecules in targeted cancer therapy: advances, challenges, and future perspectives. *Signal Transduct Target Ther*. 2021;6:201. doi:10.1038/s41392-021-00572-w
19. Meng D, He W, Zhang Y, et al. Development of PI3K inhibitors: advances in clinical trials and new strategies (Review). *Pharmacol Res*. 2021;173:105900. doi:10.1016/j.phrs.2021.105900
20. Sirico M, D'Angelo A, Gianni C, Casadei C, Merloni F, De Giorgi U. Current state and future challenges for PI3K inhibitors in cancer therapy. *Cancers*. 2023;15:703. doi:10.3390/cancers15030703
21. Castel P, Toska E, Engelman JA, Scaltriti M. The present and future of PI3K inhibitors for cancer therapy. *Nat Cancer*. 2021;2:587-597. doi:10.1038/s43018-021-00218-4
22. Mishra R, Patel H, Alanazi S, Kilroy MK, Garrett JT. PI3K inhibitors in cancer: clinical implications and adverse effects. *Int J Mol Sci*. 2021;22:3464. doi:10.3390/ijms22073464
23. Huang X, You L, Nepovimova E, et al. Inhibitors of phosphoinositide 3-kinase (PI3K) and phosphoinositide 3-kinase-related protein kinase family (PIKK). *J Enzyme Inhib Med Chem*. 2023;38:2237209. doi:10.1080/14756366.2023.2237209
24. Emran TB, Shahriar A, Mahmud AR, et al. Multidrug resistance in cancer: understanding molecular mechanisms, immunoprevention and therapeutic approaches. *Front Oncol*. 2022;12:891652. doi:10.3389/fonc.2022.891652
25. Doostmohammadi A, Jooya H, Ghorbanian K, Gohari S, Dadashpour M. Potentials and future perspectives of multi-target drugs in cancer treatment: the next generation anti-cancer agents. *Cell Commun Signal*. 2024;22:228. doi:10.1186/s12964-024-01607-9
26. Jallah JK, Dweh TJ, Anjankar A, Palma O. A review of the advancements in targeted therapies for breast cancer. *Cureus*. 2023;15:e47847. doi:10.7759/cureus.47847
27. Jan N, Sofi S, Qayoom H, et al. Metronomic chemotherapy and drug repurposing: a paradigm shift in oncology. *Heliyon*. 2024;10:e24670. doi:10.1016/j.heliyon.2024.e24670
28. Olayiwola Y, Gollahon L. Natural compounds and breast cancer: chemo-preventive and therapeutic capabilities of chlorogenic acid and cinnamaldehyde. *Pharmaceuticals*. 2024;17:361. doi:10.3390/ph17030361
29. Effiong ME, Afolabi IS, Chinedu SN. Assessing the nutritional quality of Pleurotus ostreatus (oyster mushroom). *Front Nutr*. 2024;10:1279208. doi:10.3389/fnut.2023.1279208
30. Effiong ME, Umeokwochi CP, Afolabi IS, Chinedu SN. Comparative antioxidant activity and phytochemical content of five extracts of Pleurotus ostreatus (oyster mushroom). *Sci Rep*. 2024;14:3794. doi:10.1038/s41598-024-54201-x
31. Dallakyan S, Olson AJ. Small-molecule library screening by docking with PyRx. *Methods Mol Biol*. 2015;1263:243-250. doi:10.1007/978-1-4939-2269-7_19.
32. Trott O, Olson AJ. AutoDock Vina: improving the speed and accuracy of docking with a new scoring function, efficient optimization, and multithreading. *J Comput Chem*. 2010;31:455-461. doi:10.1002/jcc.21334
33. Xiong G, Wu Z, Yi J, et al. ADMETlab 2.0: an integrated online platform for accurate and comprehensive predictions of ADMET properties. *Nucleic Acids Res*. 2021;49:W5-W14. doi:10.1093/nar/gkab255

34. Effiong ME, Bella-Omunagbe M, Afolabi IS, Chinedu SN. In silico evaluation of potential breast cancer receptor antagonists from GC-MS and HPLC identified compounds in Pleurotus ostreatus extracts. *RSC Adv*. 2024;14:23744-23771. doi:10.1039/d4ra03832k
35. Owoloye AJ, Ligali FC, Enejoh OA, et al. Molecular docking, simulation and binding free energy analysis of small molecules as PfHT1 inhibitors. *PLoS ONE*. 2022;17:e0268269. doi:10.1371/journal.pone.0268269
36. Hernández-Rodríguez M, Rosales-Hernández MC, Mendieta-Wejebe JE, Martínez-Archundia M, Basurto JC. Current tools and methods in molecular dynamics (MD) simulations for drug design. *Curr Med Chem*. 2016;23:3909-3924. doi:10.2174/0929867323666160530144742
37. Sastry GM, Adzhigirey M, Day T, Annabhimoju R, Sherman W. Protein and ligand preparation: parameters, protocols, and influence on virtual screening enrichments. *J Comput Aided Mol Des*. 2013;27:221-234. doi:10.1007/s10822-013-9644-8
38. 2021-4 SR. *Protein Preparation Wizard*. Epik, Schro¨dinger, LLC; 2021.
39. Builder P. Sytem Builder; 2022.
40. Banks JL, Beard HS, Cao Y, et al. Integrated modeling program, applied chemical theory (IMPACT). *J Comput Chem*. 2005;26:1752-1780. doi:10.1002/jcc.20292
41. Martyna GJ, Tobias DJ, Klein ML. Constant pressure molecular dynamics algorithms. *J Chem Phys*. 1994;101:4177-4189.
42. Chinedu SN, Bella-Omunagbe M, Okafor E, Afolabi R, Adebiyi E. Computational studies on 6-Pyruvoyl Tetrahydropterin Synthase (6-PTPS) of Plasmodium falciparum. *Bioinform Biol Insights*. 2024;18:11779322241230214. doi:10.1177/11779322241230214.
43. Oduselu GO, Afolabi R, Ademuwagun I, Vaughan AAE. Structure-based pharmacophore modeling, virtual screening, and molecular dynamics simulation studies for identification of Plasmodium falciparum 5-aminolevulinate synthase inhibitors. *Front Med*. 2023;9:1022429.
44. Mazurakova A, Koklesova L, Samec M, et al. Anti-breast cancer effects of phytochemicals: primary, secondary, and tertiary care. *EPMA J*. 2022;13:315-334. doi:10.1007/s13167-022-00277-2
45. Mohan Shankar G, Swetha M, Keerthana CK, Rayginia TP, Anto RJ. Cancer chemoprevention: a strategic approach using phytochemicals. *Front Pharmacol*. 2022;12:809308. doi:10.3389/fphar.2021.809308
46. Zhang HP, Jiang RY, Zhu JY, et al. PI3K/AKT/mTOR signaling pathway: an important driver and therapeutic target in triple-negative breast cancer. *Breast Cancer*. 2024;31:539-551. doi:10.1007/s12282-024-01567-5
47. Shan KS, Bonano-Rios A, Theik NWY, Hussein A, Blaya M. Molecular targeting of the Phosphoinositide-3-Protein Kinase (PI3K) pathway across various cancers. *Int J Mol Sci*. 2024;25:1973. doi:10.3390/ijms25041973
48. Neagu AN, Whitham D, Bruno P, et al. Onco-breastomics: an eco-evo-devo holistic approach. *Int J Mol Sci*. 2024;25:1628. doi:10.3390/ijms25031628
49. Pei J, Velu P, Zareian M, Feng Z, Vijayalakshmi A. Effects of syringic acid on apoptosis, inflammation, and AKT/mTOR signaling pathway in gastric cancer cells. *Front Nutr*. 2021;8:788929. doi:10.3389/fnut.2021.788929.
50. Chinnikrishnan P, Aziz Ibrahim IA, Alzahrani AR, Shahzad N, Sivaprakasam P, Pandurangan AK. The role of selective flavonoids on triple-negative breast cancer: an update. *Separations*. 2023;10:207. doi:10.3390/separations10030207.
51. Maugeri A, Calderaro A, Patanè GT, et al. Targets involved in the anti-cancer activity of quercetin in breast, colorectal and liver neoplasms. *Int J Mol Sci*. 2023;24:2952. doi:10.3390/ijms24032952
52. Bruning A. Inhibition of mTOR signaling by quercetin in cancer treatment and prevention. *Anticancer Agents Med Chem*. 2013;13:1025-1031. doi:10.2174/18715206113139990114
53. Sethi G, Rath P, Chauhan A, et al. Apoptotic mechanisms of quercetin in liver cancer: recent trends and advancements. *Pharmaceutics*. 2023;15:712. doi:10.3390/pharmaceutics15020712
54. Biswas P, Dey D, Biswas PK, et al. A comprehensive analysis and anti-cancer activities of quercetin in ROS-mediated cancer and cancer stem cells. *Int J Mol Sci*. 2022;23:11746. doi:10.3390/ijms231911746
55. Čižmáriková M, Michalková R, Mirossay L, et al. Ellagic acid and cancer hallmarks: insights from experimental evidence. *Biomolecules*. 2023;13:1653. doi:10.3390/biom13111653
56. Mohammed Saleem YI, Selim MI. MDM2 as a target for ellagic acid-mediated suppression of prostate cancer cells in vitro. *Oncol Rep*. 2020;44:1255-1265. doi:10.3892/or.2020.7664
57. Zhao J, Li G, Wei J, et al. Ellagic acid induces cell cycle arrest and apoptosis via the TGF-β1/Smad3 signaling pathway in human colon cancer HCT.116 cells. *Oncol Rep*. 2020;44:768-776. doi:10.3892/or.2020.7617
58. Wang D, Chen Q¸ Tan Y, Liu B, Liu C. Ellagic acid inhibits human glioblastoma growth in vitro and in vivo. *Oncol Rep*. 2017;37:1084-1092. doi:10.3892/or.2016.5331.
59. Vanella L, Di Giacomo C, Acquaviva R, et al. Apoptotic markers in a prostate cancer cell line: effect of ellagic acid. *Oncol Rep*. 2013;30:2804-2810. doi:10.3892/or.2013.2757.
60. Kaur H, Kaur G. A critical appraisal of solubility enhancement techniques of polyphenols. *J Pharm*. 2014;2014:180845. doi:10.1155/2014/180845
61. Hu Y, Lin Q¸ Zhao H, et al. Bioaccessibility and bioavailability of phytochemicals: influencing factors, improvements, and evaluations. *Food Hydrocoll*. 2023;135:108165. doi:10.1016/j.foodhyd.2022.108165
62. Zuccari G, Baldassari S, Ailuno G, Turrini F, Alfei S, Caviglioli G. Formulation strategies to improve oral bioavailability of ellagic acid. *Applied Sciences*. 2020;10:3353. doi:10.3390/app10103353
63. Elendran S, Shiva Kumar V, Sundralingam U, Tow WK, Palanisamy UD. Enhancing the bioavailability of the ellagitannin, geraniin: formulation, characterization, and in vivo evaluation. *Int J Pharm*. 2024;660:124333. doi:10.1016/j.ijpharm.2024.124333
64. Chen P, Chen F, Guo Z, Lei J, Zhou B. Recent advancement in bioeffect, metabolism, stability, and delivery systems of apigenin, a natural flavonoid compound: challenges and perspectives. *Front Nutr*. 2023;10:1221227. doi:10.3389/fnut.2023.1221227
65. Pais ACS, Coscueta ER, Pintado MM, Silvestre AJD, Santos SAO. Exploring the bioaccessibility and intestinal absorption of major classes of pure phenolic compounds using in vitro simulated gastrointestinal digestion. *Heliyon*. 2024;10:e28894. doi:10.1016/j.heliyon.2024.e28894
66. Ahmed Juvale II, Abdul Hamid AA, Abd Halim KB, Che Has AT. P-glycoprotein: new insights into structure, physiological function, regulation and alterations in disease. *Heliyon*. 2022;8:e09777. doi:10.1016/j.heliyon.2022.e09777
67. Patel D, Sethi N, Patel P, Shah S, Patel K. Exploring the potential of P-glycoprotein inhibitors in the targeted delivery of anti-cancer drugs: a comprehensive review. *Eur J Pharm Biopharm*. 2024;198:114267. doi:10.1016/j.ejpb.2024.114267
68. Isabel UV, de la Riera M, Belén A, Dolores RS, Elena GB. A new frontier in neuropharmacology: recent progress in natural products research for blood-brain barrier crossing. *Curr Res Biotechnol*. 2024;8:100235. doi:10.1016/j.crbiot.2024.100235
69. Hossam Abdelmonem B, Abdelaal NM, Anwer EKE, et al. Decoding the role of CYP450 enzymes in metabolism and disease: a comprehensive review. *Biomedicines*. 2024;12:1467. doi:10.3390/biomedicines12071467
70. Lee J, Beers JL, Geffert RM, Jackson KD. A review of CYP-mediated drug interactions: mechanisms and in vitro drug-drug interaction assessment. *Biomolecules*. 2024;14:99. doi:10.3390/biom14010099
71. DeRango-Adem EF, Blay J. Does oral apigenin have real potential for a therapeutic effect in the context of human gastrointestinal and other cancers? *Front Pharmacol*. 2021;12:681477. doi:10.3389/fphar.2021.681477
72. Fowler P, Bearzatto A, Beevers C, et al. Assessment of the three-test genetic toxicology battery for groundwater metabolites. *Mutagenesis*. 2024;39:146-155. doi:10.1093/mutage/gead037.
73. Thomas DN, Wills JW, Tracey H, et al. Ames test study designs for nitrosamine mutagenicity testing: qualitative and quantitative analysis of key assay parameters. *Mutagenesis*. 2024;39:78-95. doi:10.1093/mutage/gead033